Research Journal of Applied Sciences, Engineering and Technology 14(1): 10-28, 2017
DOI:10.19026/rjaset.14.3984
ISSN: 2040-7459; e-ISSN: 2040-7467

Submitted: May 13, 2016 Accepted: July 18, 2016 Published: January 15, 2017

Research Article

A Comparative Study about the Effectiveness of Observers and Bayesian Belief Networks for the Fault Detection and Isolation in Power Electronics

[1, 2]Abbass Zein Eddine, [1]Iyad Zaarour, [2] Francois Guerin, [1]Abbas Hijazi and [2]Dimitri Lefebvre
[1] Lebanese University, Hadat, Beiruth 1003, Lebanon
[2]GREAH-Université Le Havre, 25 rue Philippe Lebon, 76058 Le Havre Cedex, France

Abstract: The aim of this study is to highlight the capabilities of Bayesian Belief Network (BBN) in the domain of Fault Detection and Isolation (FDI) in DC/DC converter. Reliable electrical supplying systems are those which can provide continuously electrical energy to the consumers. This continuity requires fault free processes during all the phases of energy production, transfer and conversion. In order to achieve a fault free process it is mandatory to have an FDI system that holds on the faulty cases. In this study a Bayesian Naive Classifier (BNC) structure was selected and used as a first attempt to use BBNs for DC/DC power converter FDI.

Keywords: Bayesian naïve classifier, DC/DC power converter, fault detection and isolation, proportional observer

INTRODUCTION

In the recent decades, electrical energy has constituted the base of most scientific inventions and technological revolutions. As a result, electrical equipment has emerged as an integral part of our daily life leading to a greater demand for electrical energy and consequently, for reliable electrical supplying systems that continuously supplies the consumers with electrical energy. This continuity requires fault-free processes throughout all the phases of energy production, transfer and conversion. Concerning the conversion phase, energy converters play one of the most important roles in the electric power lifecycle. Therefore in our work we are going to focus on such equipment, especially the Zero Volt Switch (ZVS) full bridge isolated Buck converter. Such a converter is used in some topologies of Systems of Multiple Sources of Energy (SMSE) such as the one shown in Fig. 1. This DC/DC converter is used to manage the coupling and decoupling of the energy sources on the DC Bus according to the load demand and available power.

In order to achieve a fault-free process, it is mandatory to have a Fault Detection and Isolation (FDI) system that holds on the faulty cases. Fault detection and isolation methods are categorized as data-based methods which depend on identifying the system according to previously-collected data from the system itself and model-based methods which depend on determining the mathematical and physical equations of the system that need a deep understanding of causal relationships between process variables, inputs and outputs.

The authors in Berendsen *et al*. (1992) describe a method to detect faults in a four-quadrant chopper based on a parallel, average model for state estimation. A method for MOSFET faults in a ZVS full bridge isolated Buck converter using the DC link current patterns as the signatures of these faults has been proposed in Kim *et al*. (2008). In Meziane *et al*. (2015), a model-based approach FDI method was proposed, following a sliding mode observer based on a residual generation that was applied on a three-cell, power converter. In Levin *et al*. (2010), another observer-based method was developed for detection in a dual-redundant Buck converter. Gao *et al*. (2012) developed a fault detection method based on wavelet transform for DC/DC Buck converter. Moreover, in Guerin and Lefebvre (2009), a set of residuals was generated using parity space algorithm according to a variable structure state space model in order to detect sensor faults in ZVS full bridge isolated Buck converters. This study was completed in Guerin *et al*. (2011a) by using an additional measurement, depending on the use of a magnetic near-field probe.

This study discovers the capabilities of Bayesian Belief Network (BBN) as an FDI method for DC/DC power converters and as a complement for our work in Zein Eddine *et al*. (2016). A comparative study is done between the Proportional Observer (PO) as a well-

Corresponding Author: Abbass Zein Eddine, GREAH-Université Le Havre, 25 rue Philippe Lebon, 76058 Le Havre Cedex, France, Tel.: 0033-7-83823267

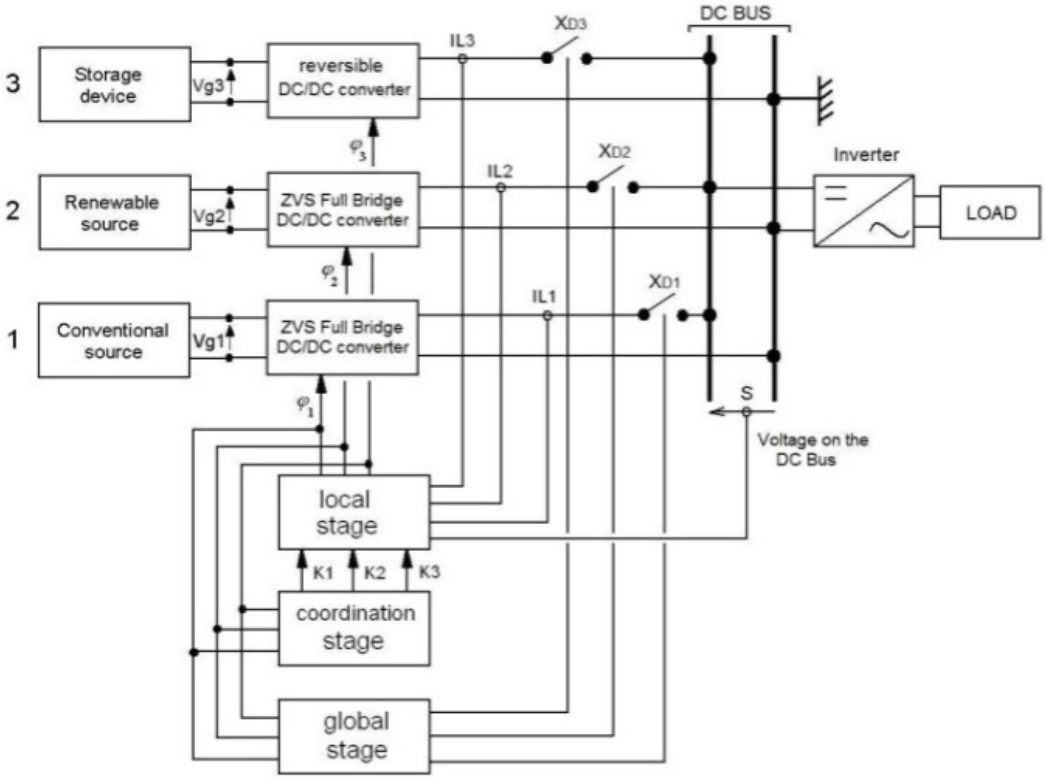

Fig. 1: Topology of the considered SMSE (Guerin *et al*., 2012)

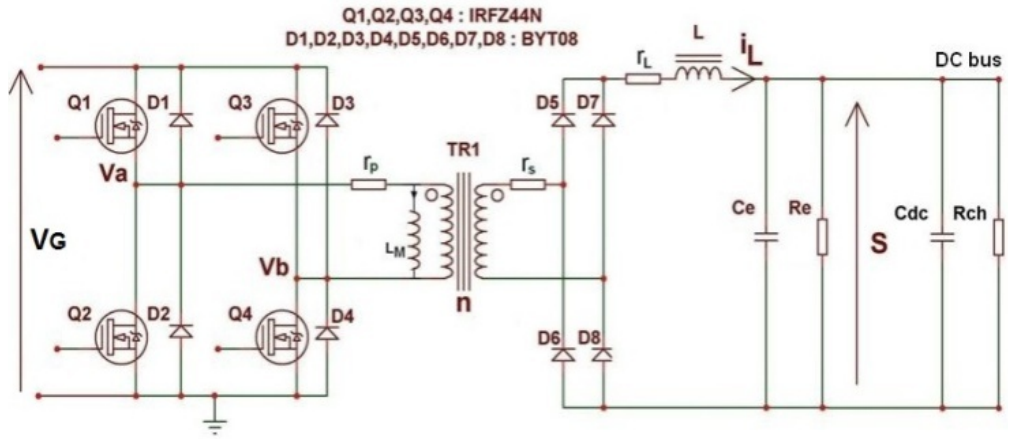

Fig. 2: Structural diagram of the ZVS full bridge isolated Buck converter

known and used FDI method versus Bayesian Naive Classifier (BNC) as a simple form of the BBN is performed. The experiment is based on real data collected from the ZVS full bridge isolated Buck converters. Open circuit faults do not often trigger fault protection but rather cause system malfunction or performance degradation. Since the standard protection systems may not detect the open circuit faults, their diagnosis becomes critical for power converters (Kamel *et al*., 2015). Hence, open circuit faults are considered in our work. The BNC overcomes the PO in both: isolation with more than 99% accuracy and simplicity while having an equal average delay approximately equal to 5 ms.

STUDIED SYSTEM AND DATA COLLECTION

Studied system: The structural diagram of the ZVS full bridge isolated Buck converter is represented in Fig. 2. These DC/DC converters are Isolated (HF transformer TR1) Buck converters (D5, D6, D7, D8, L, Ce, Re) with a full bridge and ZVS. The full bridge control (Q1, Q2, Q3, Q4) is realized by a phase shift controller UC3879 through specialized MOSFET drivers IR2113. Let us define the following variables (Table 1):

Table 1: System variables

	Symbols		
Variables	Instantaneous	Average	Measured average
Magnetizing current of the HF transformer	i_m	I_M	I_{mM}
Inductance current	i_L	I_L	I_{mL}
Source current	i_g	I_g	I_{mg}
Output voltage	s	S	S_m
Source voltage	-	-	V_G
Threshold diode voltage	V_d		

The duty cycle value φ is modified by the phase shift between V_a and V_b voltages. The phase shift is controlled by an analog DC voltage (between 0V and 5V) which represents the DC/DC converter analog voltage control input.

Four running phases must be distinguished:
Phase 1: (Q1Q4) closed: from t = 0 to t = φT_0
Phase 2: (Q1d3) closed: from t = φT_0 to t = T_0
Phase 3: (Q2Q3) closed: from t = T_0 to t = (1 + φ) T_0
Phase 4: (Q2d4) closed: from t = (1 + φ) T_0 to t = $2T_0$ = T

Mboup *et al*. (2008) and Guérin *et al*. (2011b) have developed an average state space model that depends on the duty cycle value $\varphi(t)$. Let $X_M = (I_M, I_L, S)^T$ be the state vector, $U_M = (V_G, V_d)^T$ be the input vector and $Y_M = (I_{mg}, I_{mL}, S_m)^T$ be the output vector. The average model is represented with the Eq. (1) and (2). This model will be used as a reference model in the next section in order to design the observer used for fault detection and diagnosis.

$$\dot{X}_M = A_M(\varphi(t)).X_M(t) + B_M(\varphi(t)).U_M$$
$$Y_M(t) = C_M(\varphi(t)).X_M + d(t) \quad (1)$$

where, *d(t)* represents, the measurement error vector. A_M, B_M and C_M are given by Eq. (2):

$$A_M(\varphi) = \begin{pmatrix} \frac{R_{mos}\varphi + R_{mos} + r_p}{L_M} & 0 & 0 \\ -\frac{n(2R_{mos} + r_p)}{L} & -\frac{r_L + \varphi r_s + n^2\varphi(2R_{mos} + r_p)}{L} & -\frac{1}{L} \\ 0 & \frac{1}{C_{eq}} & -\frac{1}{R_{eq}C_{eq}} \end{pmatrix}$$

$$B_M(\varphi) = \begin{pmatrix} 0 & 0 \\ \frac{n.\varphi}{L} & -\frac{2}{L} \\ 0 & 0 \end{pmatrix}, C_M(\varphi) = \begin{pmatrix} \varphi & n.\varphi & 0 \\ 0 & 1 & 0 \\ 0 & 0 & 1 \end{pmatrix}$$

$$R_{eq} = \frac{R_e R_{ch}}{R_e + R_{ch}} \; ; \; C_{eq} = C_e + C_{dc} \quad (2)$$

r_p, r_s, L_M and R_{mos} are respectively the primary resistance, the secondary resistance, the magnetizing inductance of the HF transformer (TR1) and the MOSFET transistors (Q1,Q2,Q3,Q4) channel resistance. *L*, r_L, C_e and R_e are respectively the coil inductance, the coil resistance, the capacity and the resistance of the Buck converter. *n* is the ratio of the HF transformer. R_{ch} is the load (assumed to be resistive).

Such DC/DC converters are mainly used in some topologies of Systems of Multiple Sources of Energy (SMSE) (Guerin *et al*., 2012; Guerin and Lefebvre, 2013) to couple and decouple energy sources on a DC bus according to the consumers demand and available power.

The fragility of the DC/DC converters, in addition to the environment they work in, makes them vulnerable to faults. These faults are predominantly associated with the components that form these DC/DC converters such as transistors, diodes, coils, resistors, capacitors, etc. The behavior of faulty components can be represented by a short

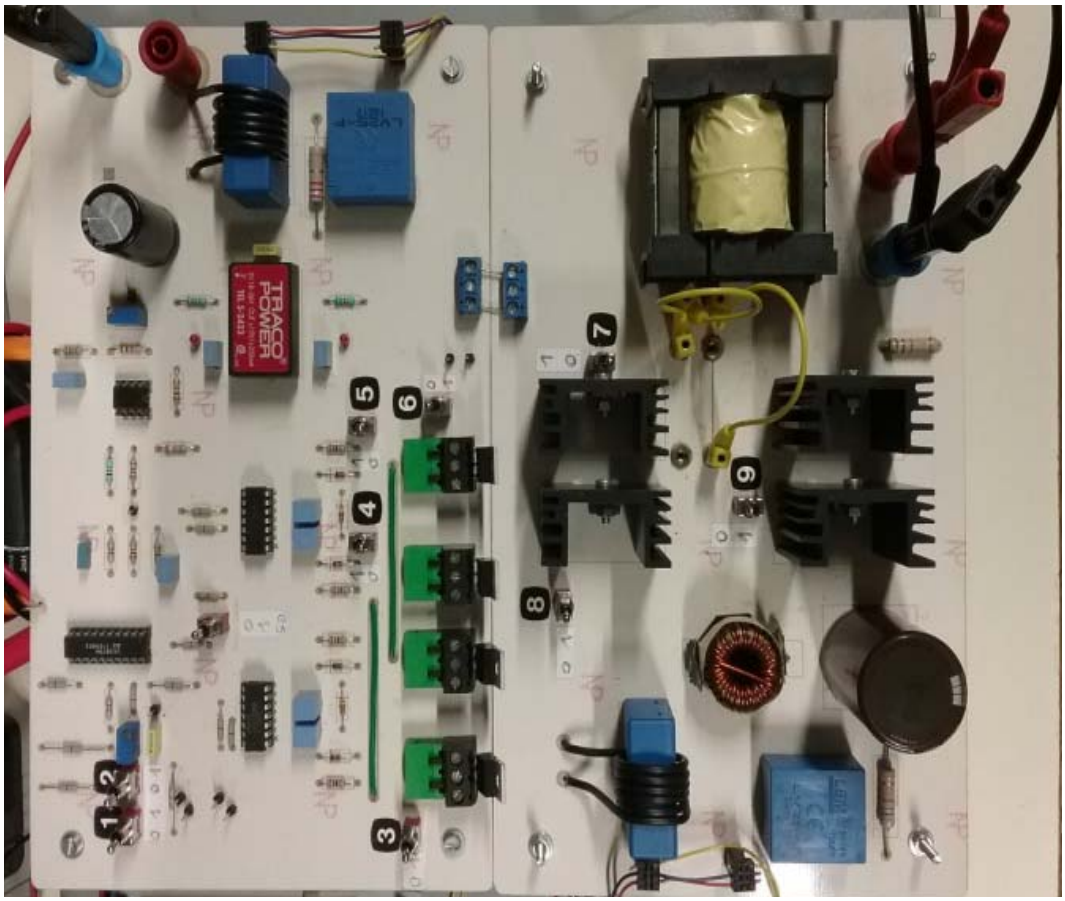

Fig. 3: ZVS full bridge isolated Buck converter designed by GREAH

circuit, an open circuit or a leakage. In this study, we study some important faults that may affect the ZVS full-bridge isolated Buck converter, particularly those related to open circuit faults. We take into consideration three main faults to be detected and isolated, fault 1: MOSFET (Q1) open circuit, fault 2: diode (D8) open circuit and fault 3: coil (L) open circuit. Let us denotefault1 by $f1$, fault 2 by $f2$, fault3 by $f3$ and the fault-free case by ff.

Data collection: Research Group GREAH, of the University of Le Havre (France), has designed and developed a ZVS full bridge isolated Buck converter (Fig. 3) with the ability to simulate ten faults, including the considered open circuit faults:

(1) Phase shift controller output stuck ON (+15V)
(2) Phase shift controller output stuck OFF (0V)
(3) MOSFET opens circuit,
(4) MOSFET driver output stuck ON (+15V)
(5) MOSFET driver output stuck OFF (0V)
(6) MOSFET short circuit,
(7) Diode short circuit,
(8) Coil open circuit,
(9) Diode opens circuit,
(10) Clock frequency deviation

This system supports our work with the required real data. In order to validate and compare the proposed methods, several series of measurements are collected in three different situations (changing the load and the source voltage values):

- Situation 1: V_G = 24 V, R_{ch}= 50 Ω
- Situation 2: V_G = 20 V, R_{ch}= 100 Ω
- Situation 3: V_G = 30 V, R_{ch}= 100 Ω

In every situation, three consecutive runs of 5 sec duration are performed consecutively, with a sampling period of $1ms$. Each run is composed of a fault-free phase followed by the occurrence of one of the considered faults. Now let us denote S_i^j as the set of the data collected (I_{mg}, I_{mL}, S_m) in run i (fault i) of the situation j. These sets are used in the learning process. Figure 4a to 4c illustrate the three consecutive runs in the learning datasets S^1, $S^2$and S^3 respectively.

In addition, for validation, other series of measurements are collected according to three scenarios, as follow:

- **Scenario 1:** it emulates $f3$ in situation 3, then $f1$ in situation 1 and finally $f2$ in situation 2.

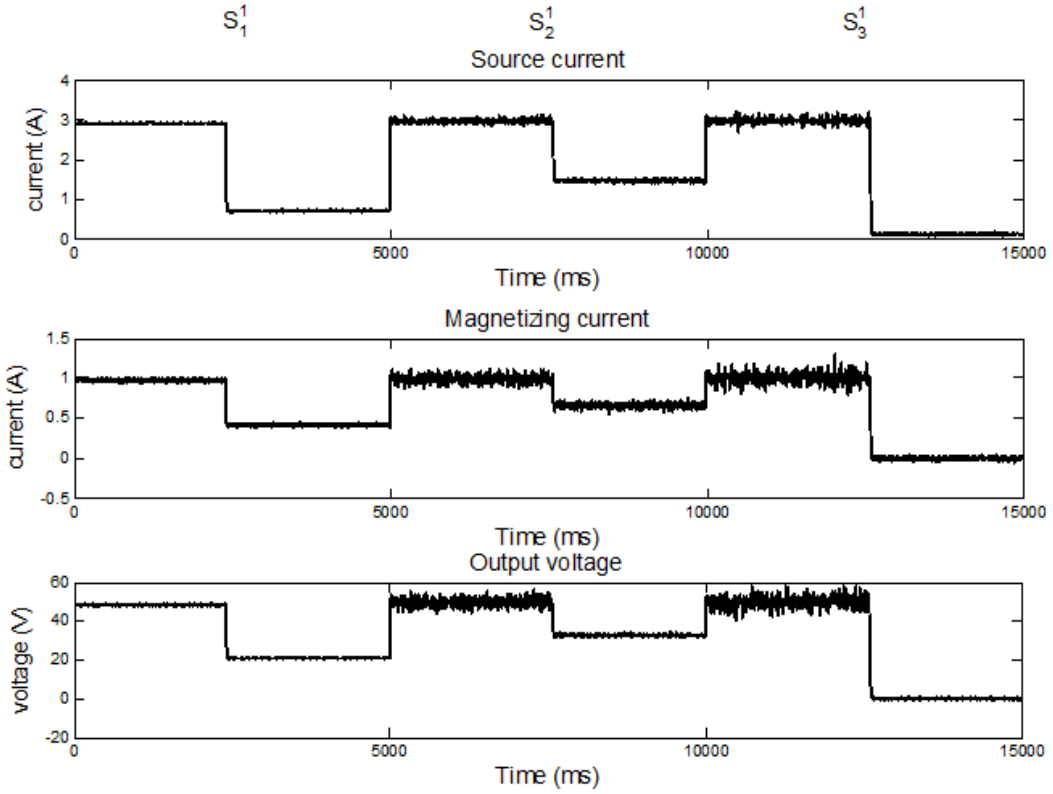
S_1^1
S_2^1
S_3^1
Source current
current (A)
Time (ms)
Magnetizing current
current (A)
Time (ms)
Output voltage
voltage (V)
Time (ms)

(a)

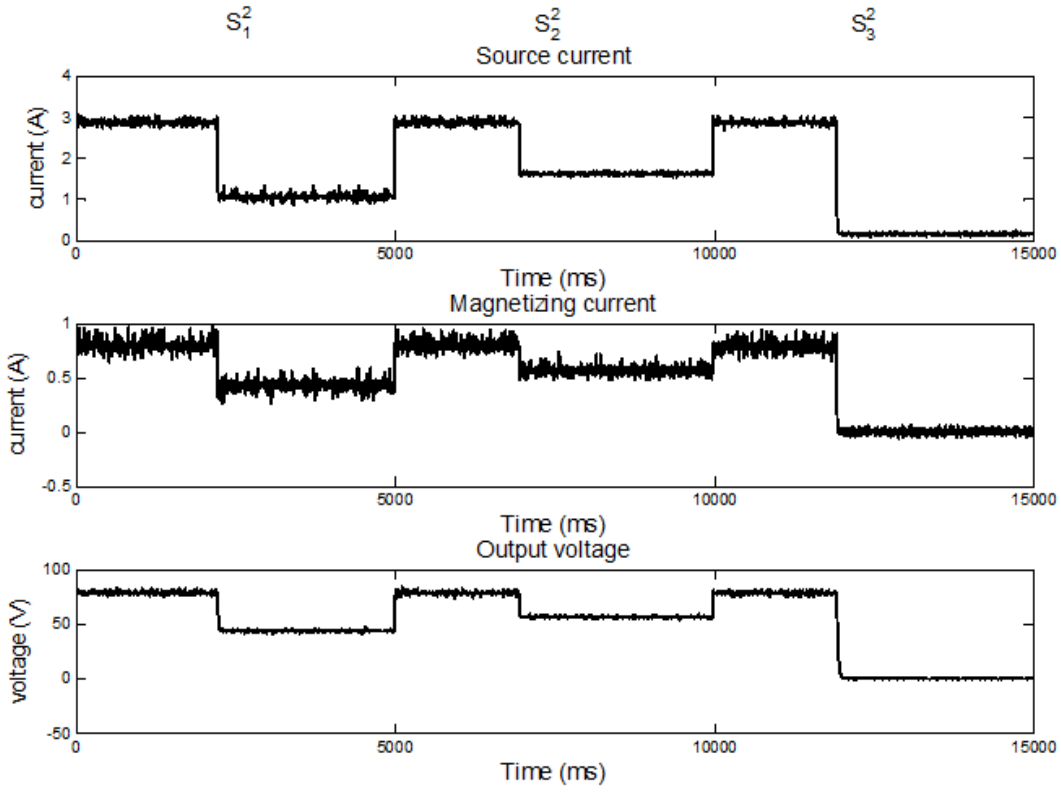
S_1^2
S_2^2
S_3^2
Source current
current (A)
Time (ms)
Magnetizing current
current (A)
Time (ms)
Output voltage
voltage (V)
Time (ms)

(b)

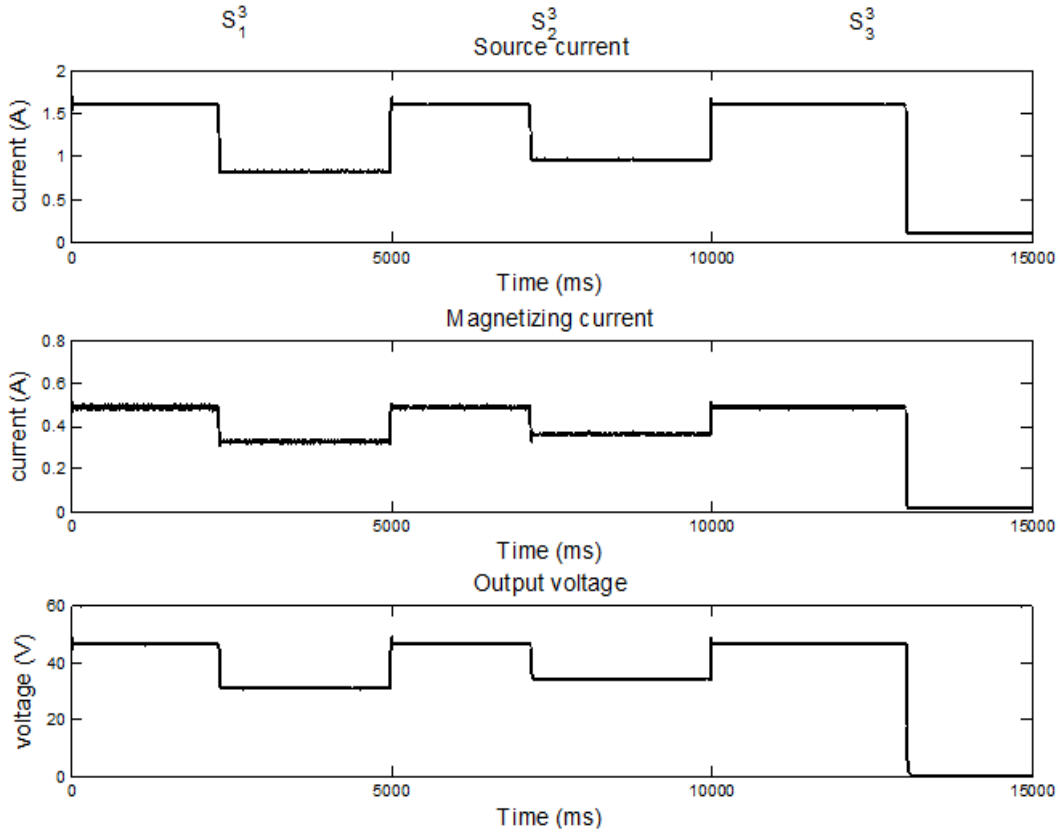

(c)

Fig. 4: Collected data; (a): Situation 1; (b): Situation 2; (c): Situation 3

- **Scenario 2:** It emulates *f*1 in situation 2, then *f*3 in situation 1 and finally *f*2 in situation 3.
- **Scenario 3:** It emulates *f*2 in situation 1, then *f*1 in situation 3 and finally *f*3 in situation 2.

Let T^i be the set of the data collected in the i^{th} scenario. These sets are represented in Fig. 5.

OBSERVER DESIGN

Luenberger's observer: The observer is basically a copy of the system with the same inputs and almost the same differential equations. The only difference is represented by an extra term that compares the actual measured output y to the estimated output $\hat{y}$, for the estimated state vector $\hat{x}$ to approach the actual state value x. The equation of the observer is given by (3):

$$\dot{\hat{X}} = A_{obs}.\hat{X}_M(t) + B_{obs}.\begin{bmatrix} U_M \\ Y_M \end{bmatrix}$$
$$\widehat{Y_M} = C_M.\hat{X}_M \quad (3)$$

With $A_{obs} = (A_M - L_{obs}C_M)$, $B_{obs} = [B_M L_{obs}]$ and L_{obs} as the observer gain.

Let us examine the estimation error $e(t) = \hat{X}_M(t) - X_M(t)$ to study how to choose the observer gain L_{obs}. The dynamics of the estimation error is given by $\dot{e}(t) = (A_M - L_{obs}C_M)e(t)$. To ensure that the error tends to zero and thus the estimated state $\hat{X}_M(t)$ rapidly and asymptotically approach $X_M(t)$, the observer gain L_{obs} is chosen such that the eigenvalues of $(A_M - L_{obs}C_M)$ are larger than those of A_M in magnitude and lie in the left-hand side of the complex plane. When the eigen values are placed at desired locations, the estimated state $\hat{X}_M(t)$ will asymptotically approach $X_M(t)$.

Residual computation: The proposed method for residual computation consists of comparing the system measured variables (I_{mg}, I_{mL}, S_m) with the estimated ones. The estimated values are generated by the observer previously-developed. The residuals are generated according to Eq. (4):

$$r(t) = y(t) - \hat{y}(t) \quad (4)$$

At each sample time, the measured values are compared to the estimated ones to get a vector $r(t)$ =

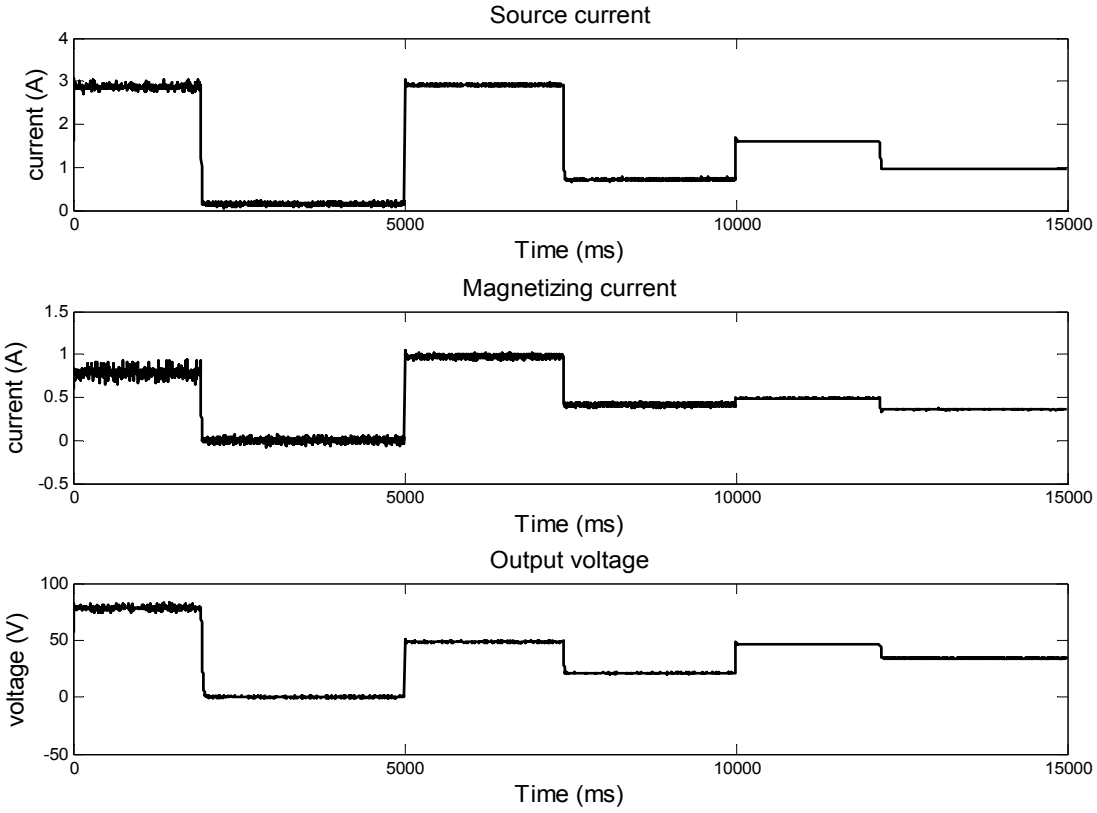
Source current
current (A)
Time (ms)
Magnetizing current
current (A)
Time (ms)
Output voltage
voltage (V)
Time (ms)

(a)

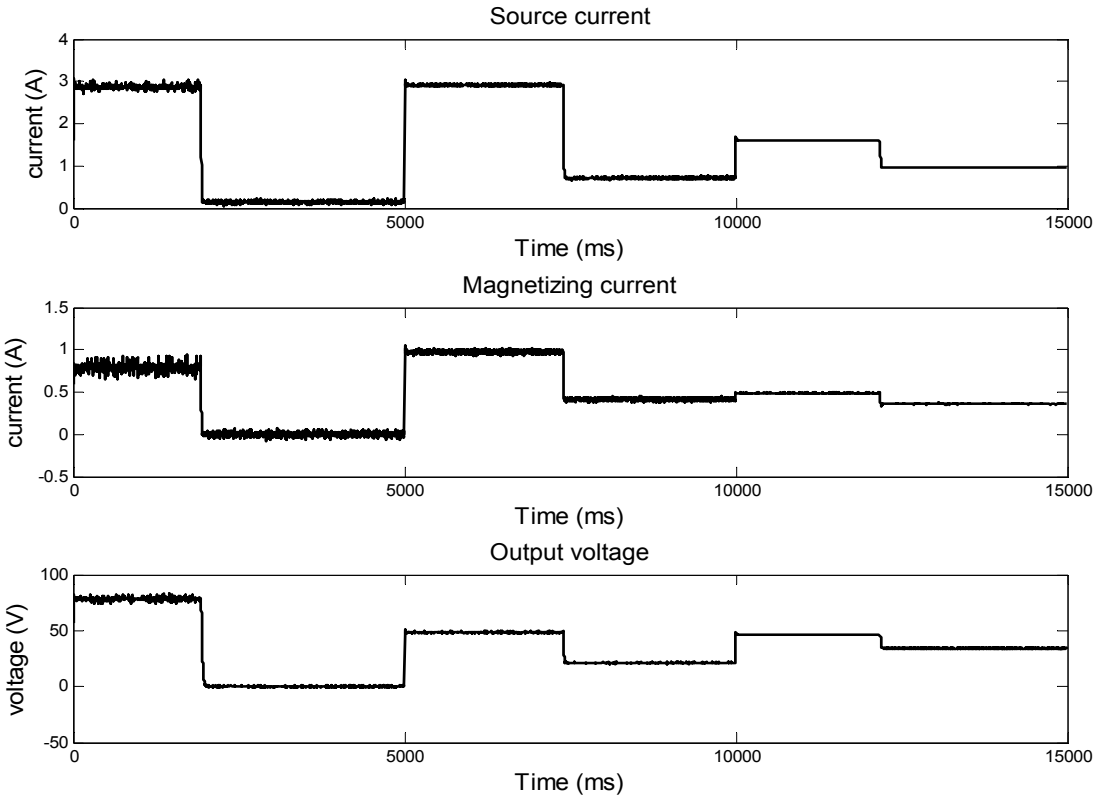
Source current
current (A)
Time (ms)
Magnetizing current
current (A)
Time (ms)
Output voltage
voltage (V)
Time (ms)

(b)

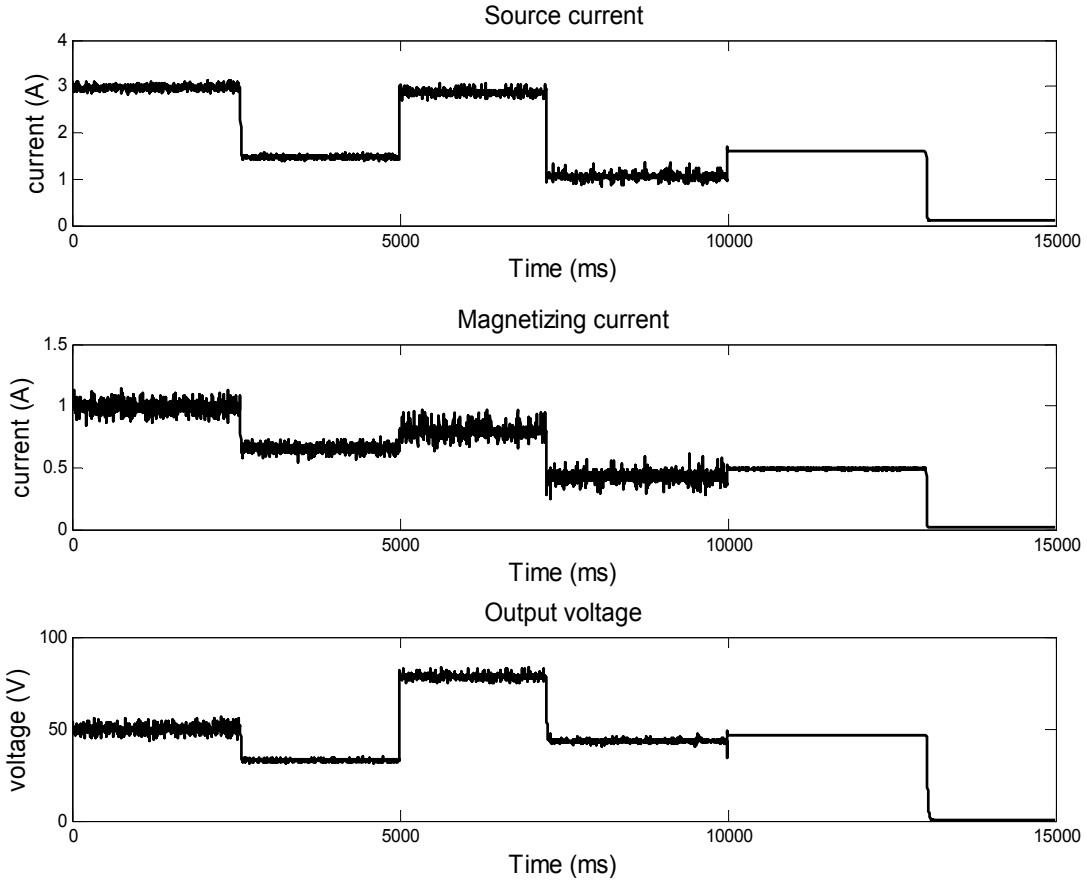

(c)

Fig. 5: Collected data; (a): Scenario 1; (b): Scenario 2; (c): Scenario 3

(r_{I_G}, r_{I_L}, r_S) of residuals. This vector will be used to detect and isolate the considered faults.

Fault detection and isolation: Fault detection stands for indicating the occurrence of faults. The occurrence of the considered faults will be reflected as a change in the state and the measured variables of the system. The comparison between the system variables and the estimated ones provided by the observer (3) will lead to several residuals. If there is no fault, the residuals will be zero in the average. On the other hand, the existence of any fault will lead to nonzero values for some of the residuals. Thus, a convenient threshold should be specified in order to detect the faults and avoid false alarms. The selected threshold is based on the standard deviation of the residuals in the fault-free case which represents the deviation of the residuals value from their mean in the normal case. This value is multiplied by again k in order to ensure that the detection is not a false alarm Eq. (5):

$$Thr = k.\sigma = k.\sqrt{\frac{\sum_{i=1}^{N}(x_i-\mu)}{N}} \quad (5)$$

where,
μ : The mean of x_i
N : The number of the measured points

This step will result in a threshold vector of three components, one for each residual component $(Thr_{r_{IG}}, Thr_{r_{IL}}, Thr_{r_S})$. Whenever one of the components is above its threshold, a fault is detected.

Experimental results: To highlight the performance of the designed observer, it is tested with the real data collected (Fig. 4) from the designed DC/DC converter (Fig. 3). The observer is used to estimate the state and the output of the real system. Those estimated values are then compared to the real values to generate residuals. Subsequently, the generated residuals are analyzed using a simple comparison with the calculated threshold in order to detect and isolate faults. Figure 6 shows the generated residuals and the detection alarm. It is clear that the observer was able to detect the three fault sin all the situation with a short delay. Table 2 sums up the occurrence and detection time in addition to the delay of detection.

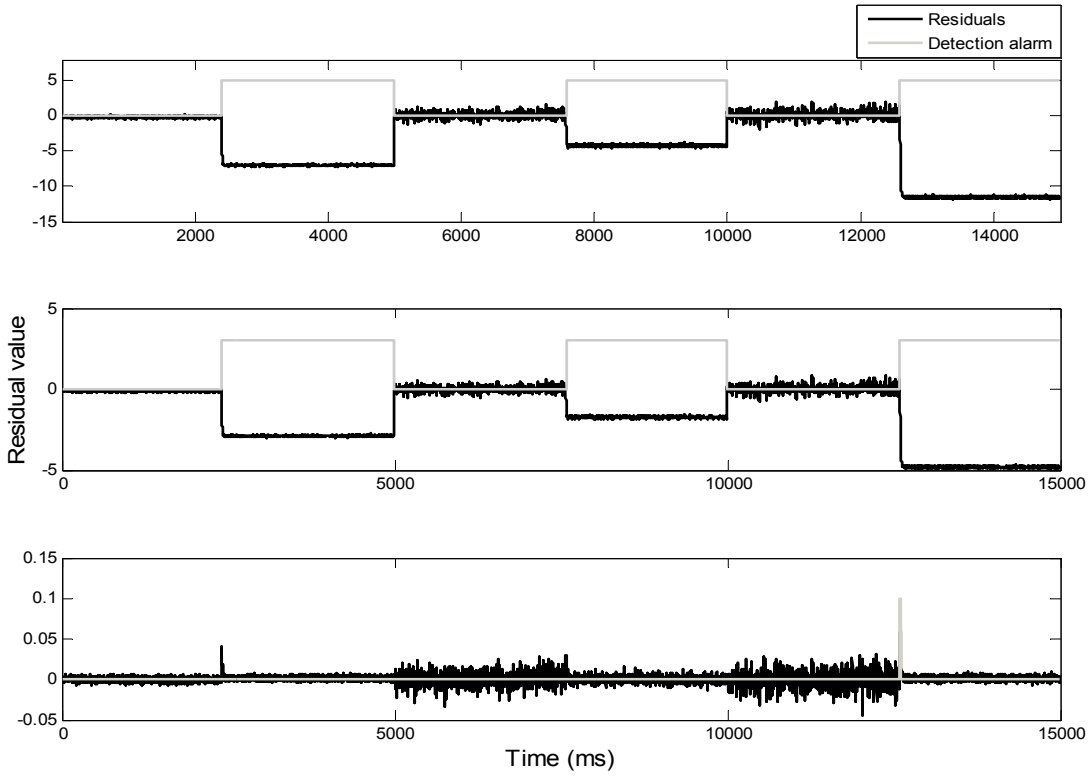
Residuals
Detection alarm
Residual value
Time (ms)

(a)

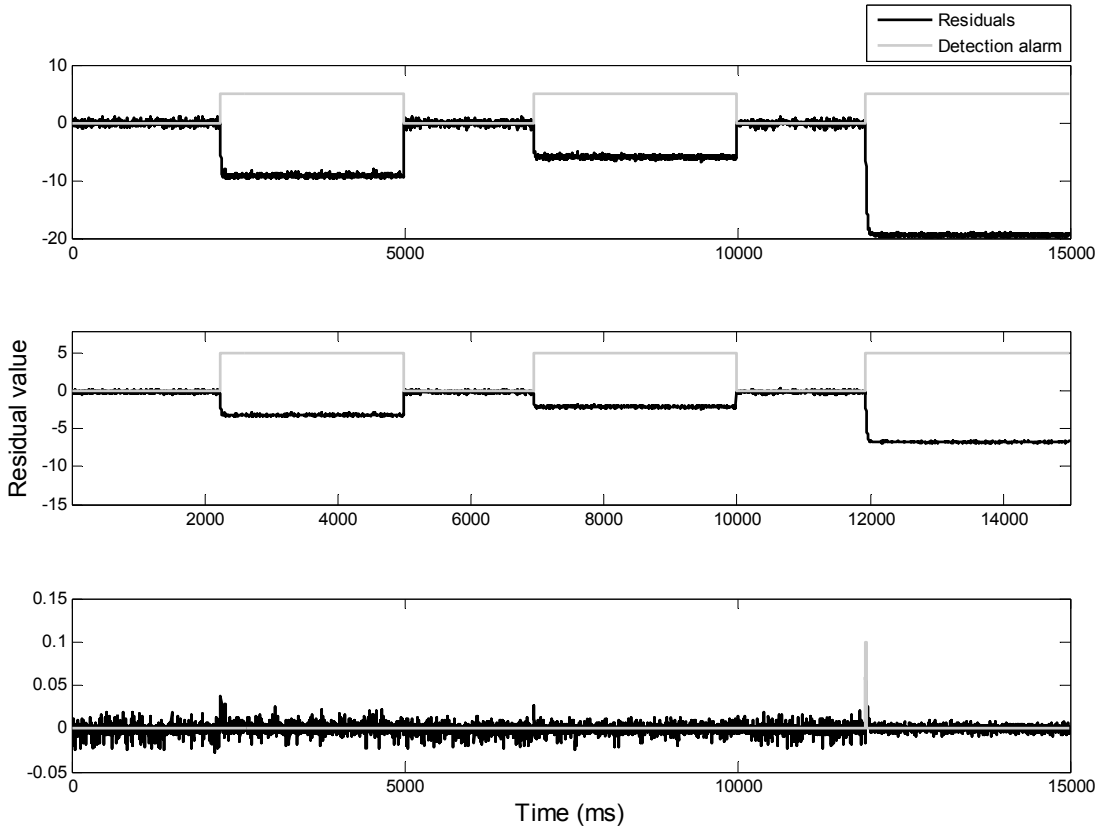
Residuals
Detection alarm
Residual value
Time (ms)

(b)

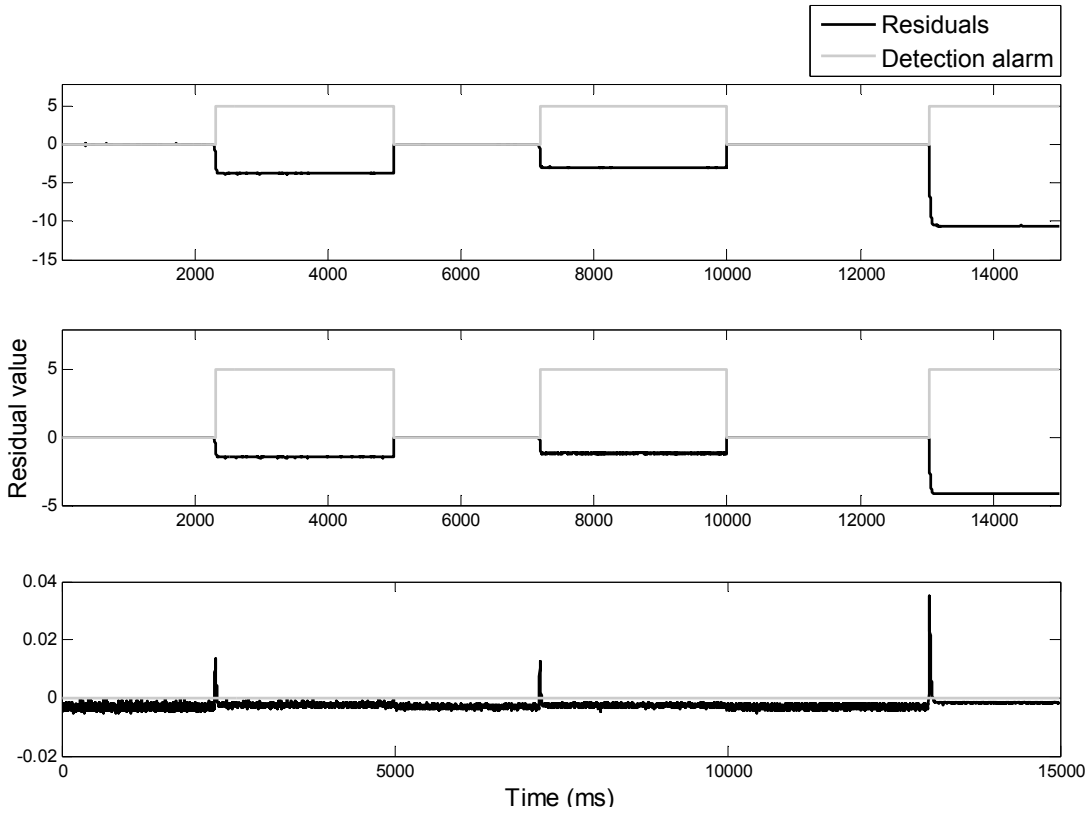

(c)

Fig. 6: Residuals (Source current I_G, Inductance current I_L, Output voltage S); (a): Situation 1 residuals and detection alarm; (b): Situation 2 residuals and detection alarm; (c): Situation 3 residuals and detection alarm

Table 2: Delay for detection with PO

Situation	Faults	Occurrence time (sec)	Detection time (sec)	Delay (ms)
Situation 1	Fault 1	2.3930	2.3980	5
	Fault 2	7.5680	7.5760	8
	Fault 3	12.587	12.591	4
Situation 2	Fault 1	2.2300	2.2340	4
	Fault 2	6.9370	6.9420	5
	Fault 3	11.928	11.928	3
Situation 3	Fault 1	2.3090	2.3150	6
	Fault 2	7.1890	7.1950	6
	Fault 3	13.030	13.032	2

The main problem is that the three faults are not isolable because the signature of the 3 faults is similar (Table 3). Consequently, other characteristics which need more signal processing should be studied. Otherwise, additional methods should be used such as data mining and machine learning methods.

Table 3: Fault signatures

Residuals	R_{IG}	R_{IL}	R_S
Fault 1	-	-	0
Fault 2	-	-	0
Fault 3	-	-	0

BAYESIAN BELIEF NETWORK

Bayesian Belief Network (BBN) is a powerful tool of knowledge representation and inference under the uncertainty framework (Jensen, 1996; Pearl, 1988). In addition, it is a perfect representative tool for probability distribution over a set of variables that are used for building a model.

These networks are defined by specifying their qualitative and quantitative components. The BBN structure (qualitative) is made of nodes that represent the random variables and arcs for the dependency between the nodes, in the form of Direct Acyclic Graph (DAG). It can be specified by experts (Wiegerinck, 2005), by structure learning algorithms that study the correlation between the nodes (studied variables) (Friedman *et al*., 1997; Pearl, 2000), or by both experts and structure learning as in Flores *et al*. (2011).

The BBN parameters (quantitative), i.e., the Conditional Probability Tables (CPT's), are filled with conditional probabilities for each node giving its parents. In general, those parameters are estimated (fully or partially) via learning processes from historical data that are either previously collected from the system or generated by system model (i.e., mathematical and physical equations representing the system) or by expert's knowledge.

These networks rely on inference algorithms to compute beliefs in the context of observed evidence (Huang and Darwiche, 1994). Inference is the process of updating the probabilities of outcomes (CPTs) based upon the relationships in the model and the evidence known about the situation at hand. Inference algorithms can be exact or approximated (Guo and Hsu, 2002).

Currently, BBNs still represent a usable subject and an attractive method in many disciplines such as finance (risk evaluation), network diagnosis as in Khanafer *et al*. (2008), fault detection as in Volosencu and Curiac (2010) and medical domains as in Bartram and Mahadevan (2013) and Saad *et al*. (2013).

Bayesian Naive Classifier (BNC): The aim of this study is to investigate the capabilities of BBN in the FDIof power electronics and to assess its performance compared to the previously designed observer. Hence, in order to highlight BBN capabilities, we assume that the BBN structure will depict a simple correlation between the direct measurement of the system output variables (I_{mg}, I_{mL}, S_m) and a decision node (fault type). Specifically, we tend to use the Bayesian Naive Classifier (BNC) as a first attempt to use BNNs for DC/DC power converter fault detection and isolation. It has been successfully applied in variousdomains of classification, such as intrusion detection, image and pattern recognition, medical diagnosis, loan approval and bioinformatics (Zaarour *et al*., 2015). Moreover, it was the subject of a particular attention in the context of the supervised classification (Tiplica *et al*., 2006). Its performance was compared to other well-known classification statistical methods (Langley *et al*., 1992; Madden, 2003). The BNC assumption that the attributes are independent, given the classification node, is surprisingly effective (Langley *et al*., 1992).

In Zein Eddine *et al*. (2015), we present an approach to detect and isolate open circuit faults in Zero Voltage Switching (ZVS) full bridge isolated Buck converters. The estimated state variables obtained with an observer were compared to measured state variables in order to generate residuals. The generated residuals were able to detect the faults but unable to isolate them. Consequently, a BNC learned from those residuals was designed in order to isolate the occurring fault. The proposed technique was able to detect the studied faults regardless of disturbance and to isolate the fault type with 99.7 % accuracy. This study was done using simulated data collected from MATLAB/Simulink after modelling the considered faults.

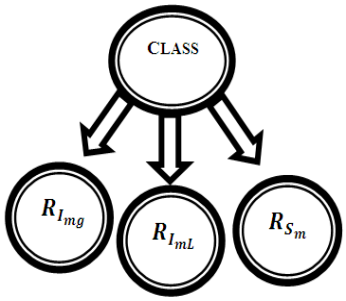

Fig. 7: Used BNC structure for isolation

Using the methodology followed in Zein Eddine *et al*. (2015), we will manipulate the same BNC structure, but this time with real data, for isolation. After that, we will use another BNC for detection and isolation at the same time.

Experimental results: Two experiments are performed. In both of them, the Naive structure is used. The parameters are learned using maximum likelihood algorithm (Redner and Walker, 1984; Grossman and Domingos, 2004) and the junction tree algorithm is used as one of the most popular exact inference algorithms (Cowell, 1998).

The first experiment is based on the work done in Zein Eddine *et al*. (2015) by using the BNC (Fig. 7) for isolation, but this time using real data, in order to support our previous work and highlight the BNC capabilities as a complementary tool. The second experiment is to use a BNC for both detection and isolation based on the direct output measurements.

In the first experiment, the BNC is used to isolate faults detected by the observer. Therefore, let us define S_R^1, S_R^2 and$S_R^3$to be the set of residuals generated during situation 1, situation 2 and situation 3 respectively (Fig. 6). These datasets are treated offline. First, the sets are discretized (Colot *et al*., 1994). Then, all residuals are labelled according to their real class type: fault free, fault1, fault2 or fault3.

Denote by F_R^1, F_R^2 and F_R^3 the sets of residuals that belong to the faulty case in each of S_R^1, S_R^2 and S_R^3 respectively. Subsequently, this part of data will be used for the BNC learning.

The process of isolation is based on inference which is the calculation of any combination of variables given any observation ($P(X/O)$ where X is a set of random unknown variables represented by the nodes in the BBN and O is the set of observed variables usually equal to$\bar{X}$). The residuals collected after the fault detection (observations) are passed through the learned BNC. The BNC in its turn will give each observation the probability for each class value (fault1, fault2 or fault3). This procedure will result in three probabilities

Table 4: Isolation Belief Index (BI)

Scenario	Faults	1st detection	2nd detection	3rd detection
Scenario 1	Fault 1	0.0069	0.9935	0.0466
	Fault 2	0.0025	0.0047	0.9478
	Fault 3	0.9906	0.0018	0.0056
Scenario 2	Fault 1	0.9736	0.0049	0.0099
	Fault 2	0.0244	0.0024	0.9839
	Fault 3	0.0019	0.9927	0.0062
Scenario 3	Fault 1	0.0073	0.9924	0.0094
	Fault 2	0.9903	0.0027	0.0028
	Fault 3	0.0025	0.0049	0.9878

Table 5: Confusion matrices

Scenario	True faults	Decision: fault 1	Decision: fault 2	Decision: fault 3
Scenario 1	Fault 1	2592	151	18
	Fault 2	13	2652	8
	Fault 3	2	5	3054
Scenario 2	Fault 1	2673	11	12
	Fault 2	16	3045	6
	Fault 3	1	4	2390
Scenario 3	Fault 1	2753	15	23
	Fault 2	6	2407	5
	Fault 3	6	8	1931
Total	Fault 1	8018	177	53
	Fault 2	35	8104	19
	Fault 3	9	17	7375

that correspond to each fault's responsibility for this observation.

Let A be the set of recorded residual observations.

$$A = \{r(t) = (r_{I_{mg}}, r_{I_{mL}}, r_{S_m}) \ / t \in [0, \ldots, n] \} \quad (6)$$

where, 0 is the time when fault is detected and n is the final time.

Let B be the probability of occurrence of each fault given an observation of residuals at time t.

$$B = \{p(t) = \left(P_{f_1}, P_{f_2}, P_{f_3}\right) \text{ such that } P_{f_i} = P(f_i/r(t)) \ with \ r(t) \in A \ and \ i \in [1,2,3]\} \quad (7)$$

The calculated probabilities will be the core of the isolation process:

For each *p(t)* let *c(t)* = f_1 if *max(p(t))*= $P_{f_1}(t)$, *c(t)* = f_2 if *max(p(t))*= $P_{f_2}(t)$ or *c(t)* = f_3 if *max(p(t))*= $P_{f_3}(t)$

Let C be the set of values that represent the most probable fault responsible for each observation defined as follows:

$$C = \left\{f_i \ / \ P_{f_i} = \max(P(t)) \text{ and } P(t) \in B\right\} \quad (8)$$

The fault that is isolated will be the most frequent one in set C.

In order to validate this isolation process using real data, we will consider the three scenarios T^1, T^2 and T^3. In section 3, we have noticed that the observer is able to detect the three faults in the three different situations. In each scenario, three faults are simulated. After each detection, the BNC will start to classify the recoded residuals for isolation. Hence, let T_R^1, T_R^2 and T_R^3 be the residuals generated for T^1, T^2 and T^3 respectively. In addition, let us denote by A_1, A_2 and A_3 the recoded residuals taken from $T_R^1 T_R^2$ and T_R^3 respectively, after each fault detection.

Subsequently, for each point *r(t)* in A_1, A_2, or A_3, *r(t)* is fed to the BNC. The BNC will return a value:

$$p(t) = \{P_{f_1}(t) = P(f_1/r(t)), P_{f_2}(t) = P(f_2/r(t)), P_{f_3}(t) = P(f_3/r(t))\}$$

Let B_1, B_2 and B_3 be the set of probabilities according to A_1, A_2 and A_3 respectively (equation 7). A meaningful value can be computed from those probabilities, which is the Belief Index (BI). This value evaluates how accurate the BNC decision is (decision confidence) and thus insures whether it's a false alarm or not. BI is represented by the mean of the probabilities of each fault after each detection in every B_i set (9):

$$BI_{f_i} = \frac{\sum_{j=1}^{N} (P_{f_i}(t))_j}{N} \quad (9)$$

where, $P_{f_i}(t) \in B_i$ and N the number of recorded points after detection.

Table 4 shows the *BI* values in every scenario after each detection. These values give a very high confidence to the BNC classification.

Let C_1, C_2 and C_3 be the set of the most probable fault for each element of B_1, B_2 and B_3 respectively (equation 8).These sets are illustrated by the dashed line marked with point in Fig. 8 while the actual fault type is represented bya dashed line. It is clear that in the three graphs, both lines are almost coincident which means

that the observations are correctly classified. Table 5 shows the respective confusion matrix of each graph in Fig. 8.

The confusion matrices explain the graphs more. As an instance let us consider the first graph (scenario1), in C_1after the first detection alarm which is

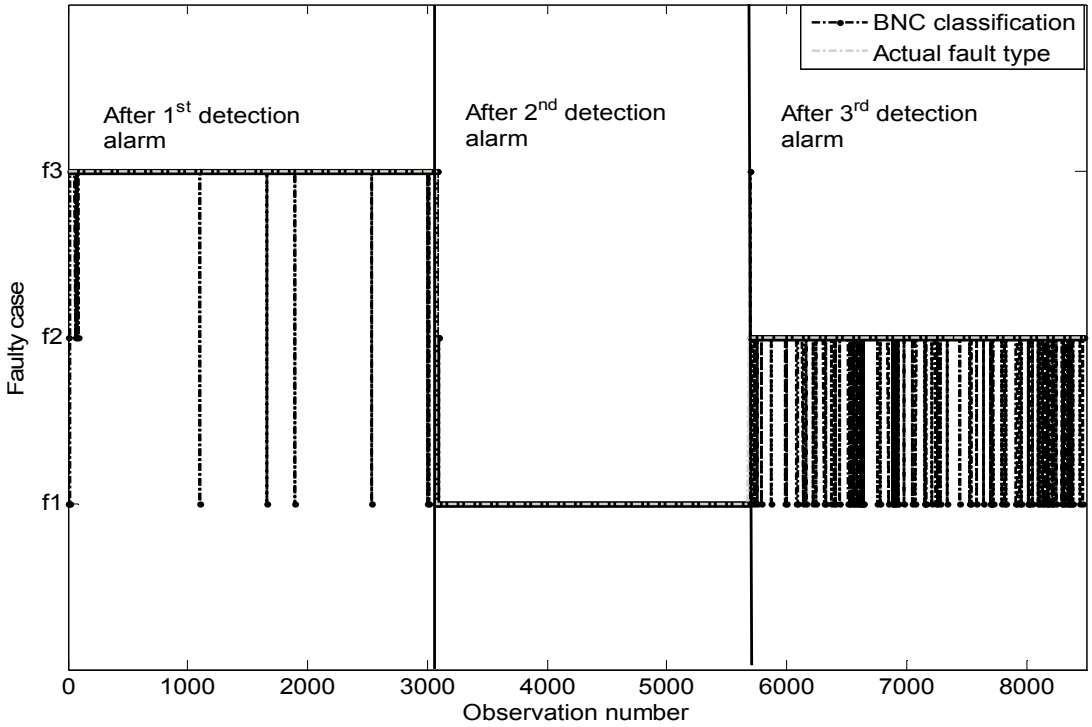

(a)

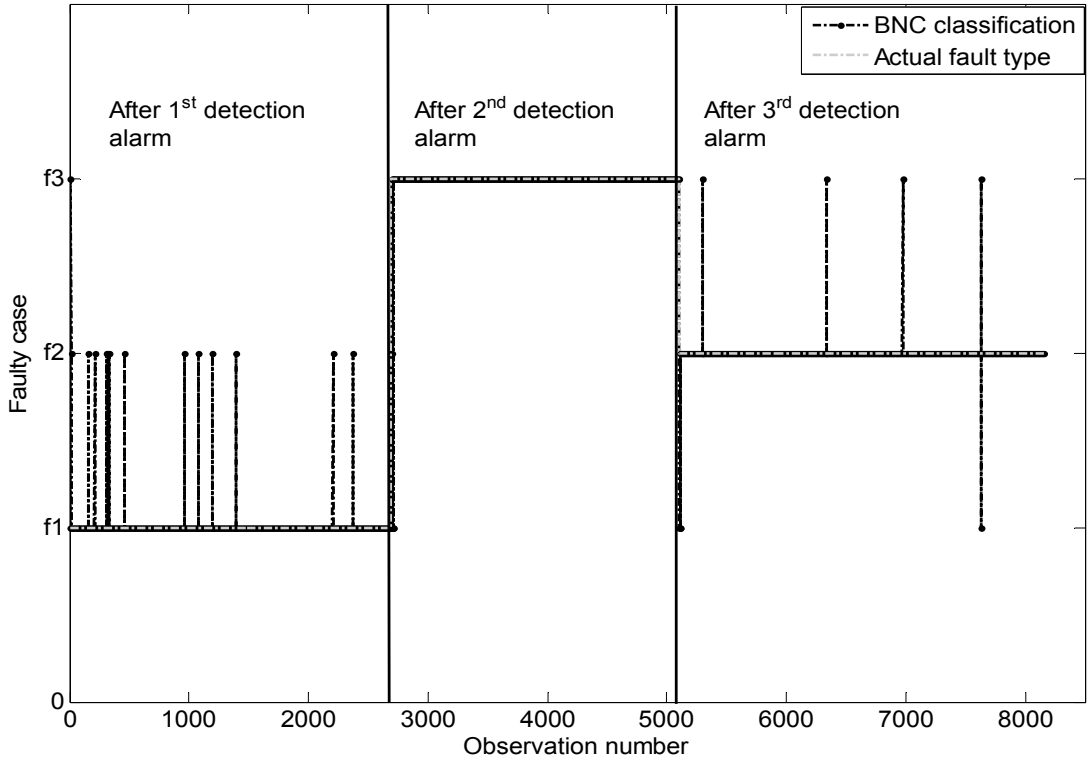

(b)

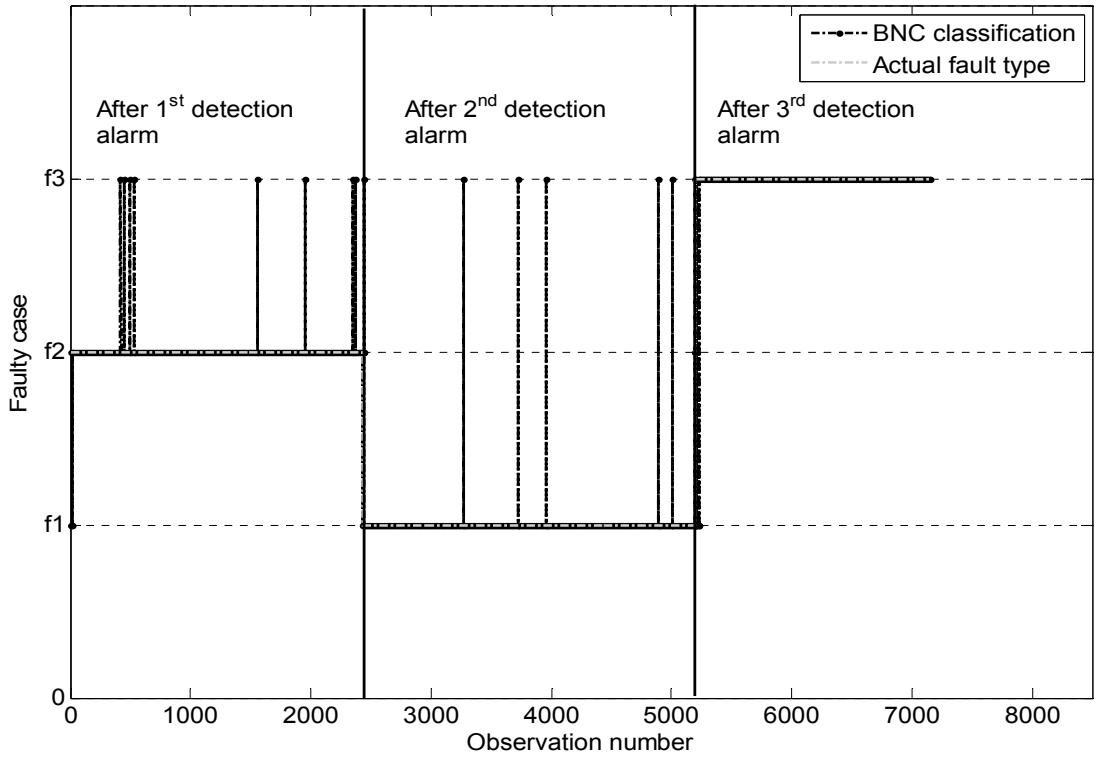

Fig. 8: BNC classifications

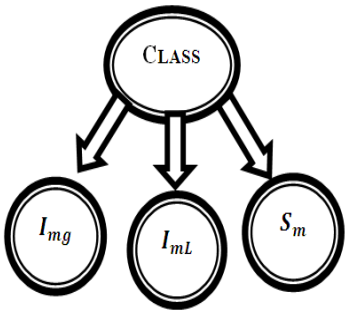

Fig. 9: Used BNC Structure for detection and isolation

actually the detection of fault 3. 18 points are classified as fault1, 8 points as fault 2, while 3054 points are classified as fault 3. Furthermore, in the third graph and at the second detection alarm which is actually for fault 1, 2673 points are correctly classified as fault 1 while only 12 points are misclassified. Those numbers represent the frequency of each fault. Now, we can say that f_i occurs (isolated) if and only if f_i is the most frequent item in the *C* set. Finally, we can calculate the accuracy of the BNC classifications by dividing the total number of correct classifications over the total number of the classified points to get an accuracy of 98%.

The second experiment reflects more clearly the independence and the efficiency of the BNC by eliminating the observer and using only the BNC for both detection and isolation.

The BNC structure shown in Fig. 9 is similar to that used in the previous experiment, except that the leaf nodes represent the direct measured outputs (I_{mg}, I_{mL}, S_m) instead of their residuals $(r_{I_G}, r_{I_L}, r_S)$and the class node can take four values instead of three. As for the parameter learning, the direct measurements taken in the three situations (S^j) are used.

At the beginning, these sets are labeled offline by adding the actual class of each point. Then, they are used for learning the Conditional Probability Tables (CPT's).

After parameter learning, the BNC is ready for inference. For validation, the three scenarios (T^i) are used. Each observation, $d(t) = (I_{mg}, I_{mL}, S_m)$ in $T^i$is passed through the BNC which in its turn will compute the probability *p(t)* of the responsibility of each fault for the given observation *d(t)*:

$$p(t)=\{P_{free}(t) = P\left(f_{free}/d(t)\right), P_{f_1}(t)(f_1/d(t)), P_{f_2}(t) = P(f_2/d(t)), P_{f_3}(t) = P(f_3/d(t))\}$$

The case with maximum probability will be considered as the BNC classification. Based on this immediate classification and to prevent false alarms, the detection is performed according to a window. The size of this window is chosen according to several test respecting two rules: (1) avoiding false alarms and (2)

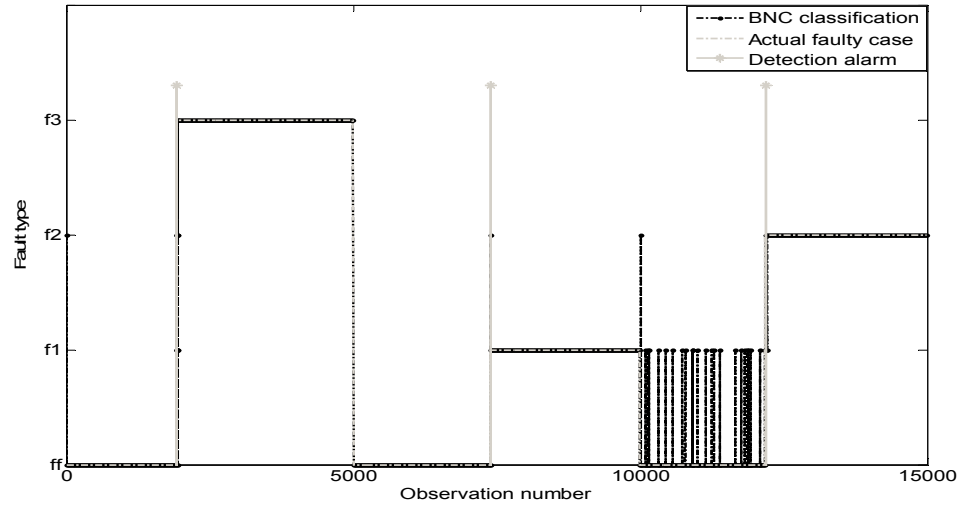

(a)

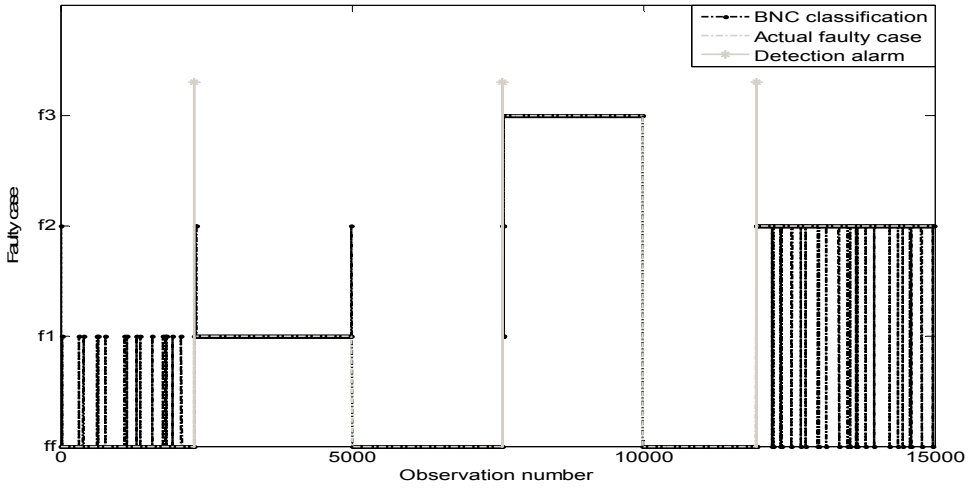

(b)

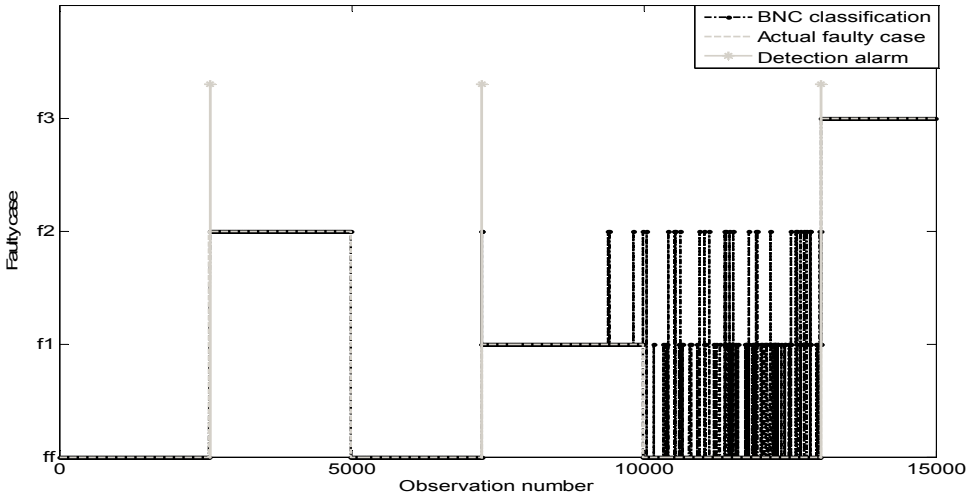

(c)

Fig. 10: BNC classification, detection and isolation

Table 6: Delay for detection with BNC

Scenario	Faults	Occurrence time (sec)	Detection time (sec)	Delay (ms)
Scenario 1	Fault 1	1.9290	1.9340	5
	Fault 2	7.3910	7.3970	6
	Fault 3	12.183	12.191	8
Scenario 2	Fault 1	2.3010	2.3040	3
	Fault 2	7.5900	7.5940	4
	Fault 3	11.940	11.945	5
Scenario 3	Fault 1	2.5690	2.5760	7
	Fault 2	7.2260	7.2300	4
	Fault 3	13.031	13.034	3

Table 7: Confusion matrices

Scenario	True fault	Decision: Fault free	Decision: fault 1	Decision: fault 2	Decision: fault 3
Scenario 1	Fault free	6475	3	0	4
	Fault 1	22	2599	18	9
	Fault 2	2	5	2799	4
	Fault 3	0	0	0	3054
Scenario 2	Fault free	6808	0	29	1
	Fault 1	18	2691	0	6
	Fault 2	1	8	3031	4
	Fault 3	0	0	0	2397
Scenario 3	Fault free	7703	0	4	0
	Fault 1	95	2758	0	5
	Fault 2	27	13	2425	6
	Fault 3	0	0	0	1958
Total	Fault free	20986	3	33	5
	Fault 1	135	8048	18	20
	Fault 2	30	26	8255	14
	Fault 3	0	0	0	7409

Table 8: Isolation belief index

Scenario	True fault	Decision: fault free	Decision: fault1	Decision: fault 2	Decision: fault 3
Scenario 1	Fault free	0.9918	0.0013	0	0.0011
	Fault 1	0.0033	0.9965	0.0065	0.0027
	Fault 2	0.0049	0.0022	0.9935	0.0017
	Fault 3	0	0	0	0.9945
Scenario 2	Fault free	0.9917	0	0.0108	0
	Fault 1	0.0038	0.9970	0	0.0025
	Fault 2	0.0044	0.0028	0.9891	0.0014
	Fault 3	0	0	0	0.9956
Scenario 3	Fault free	0.9741	0	0.0017	0
	Fault 1	0.0099	0.9944	0	0.0027
	Fault 2	0.0159	0.0050	0.9982	0.0021
	Fault 3	0	0	0	0.9951

minimizing the detection delay. Finally, the window size is selected to be equal to five, such that whenever five consecutive faulty classified points (i.e., *f*1, *f*2 or *f*3) occur, a fault is detected.

The set of recorded points after fault detection will be used for isolation. Thus, letB_i be the sets of *p(t)*'s for the *d(t)* points that belong to in T^i. From each of these sets, another equivalent set (C_i) is generated such that:

c(t)=

$$\{f_i/P_{f_i}(t) = \max(p(t)) \; where i = 1,2,3 \; or free\}$$

This process will lead to three sets (C_i) that will be used for isolation. In each set, the frequency of each f_i will be computed and the fault with the maximum frequency will be selected as the isolated fault.

The results of the discussed process are shown in Fig. 10 for the three scenarios. It's clear that the proposed BNC algorithm is able to detect and isolate the three faults in the three scenarios with high accuracy. The points actually related to the free-fault case are almost all correctly classified. Similarly, in the remaining faulty cases, a few numbers of points are misclassified. The graphs are explained more in the confusion matrix (Table 6).

For an instance, let's consider Fig. 10b. First, for detection, it's clear that the three faults are detected. At the beginning, fault 1 is detected at t = 2.304 s after 3 ms of occurrence, then fault 3 is detected at t = 7.594 s after 4 ms of its occurrence and finally fault 2 is detected after 5 ms of its occurrence at time t= 11.940s. Table 6 shows more information about occurrence time, detection time and delay for all the scenarios. Second, for isolation, the set of points recorded after this detection are classified (C_i sets). For example, let us consider in Fig. 10b the third detection at t=11.946 s. The BNC classifications are shown in dashed line marked with point while the actual fault type is

represented by a dashed line. These two lines indicate that the BNC classifications are compatible with the actual fault type in most cases.

The confusion matrix (Table 7) gives more clarification of this compatibility. In the confusion matrix of "scenario 2" in the column of fault 2 which is the third detected fault, 3031 points are classified as fault 2 (most frequent) while only 29 points are misclassified as fault free. Thus we can say that the frequency fault 2 is the greatest and the isolation decision is fault 2 which is, in fact, true. The decision of the BNC is supported by the BI calculated according to equation 9. BI results are illustrated in Table 8. From these results, fault 2 is isolated with BI = 98.9% which gives high confidence to the isolation result. In addition, the probability of having a false alarm (i.e., probability of fault free) is equal to 1.08% which insures that the detection was correct.

PO VS BNC

The aim of this study is to introduce the BNC as an efficient method for Fault Detection and Isolation (FDI) in DC/DC power converters via a comparison with Proportional Observer (PO). As an FDI method, three aspects should be taken into consideration. The first aspect is the latency of detection, the second aspect is the accuracy of isolation and the last is the simplicity of the method. For the first aspect, PO detects the three faults in an average of approximately 5 *ms* delay as can be computed from Table 4. On the other hand, for the BBN, the three considered faults are detectable as shown before. In addition, Table 6 shows an average delay time also equal to 5 *ms*. As for the second aspect which is isolation, for the PO, it is impossible to isolate the three faults using simple residual analysis while BBN shows a very high aptitude in isolation. In the first experiment, where the BNC is used as a complementary method learned from the residuals generated by the PO, all the three faults are easily and totally isolated following our isolation strategy discussed before. The reason is that, in each case, less than 5% of the points are misclassified. This isolation process is also supported by a very high confidence (about 99%). Similarly, for the second experiment where the BNC is learned from the direct measurements, all the faults are isolated with more than 99% accuracy, along with a very high confidence (BI) (Fig. 10, Table 7 and 8). Finally, the simplicity of the method is the last aspect. BNC is the simple form of BBNs and its complexity is studied in Zheng and Webb (2005). Actually, in our case, the time complexity of the learning phase will not be considered because it is done offline. What we are interested in is the time complexity of classifying a single point (observation) which equals to $O(kl)$ where k is the number of the class values and l is the number of attributes. In our case, $k = 4$ and $l = 3$, then $O(kl) = O(12)$. On the other hand, the proportional observer complexity is equal to the complexity of the matrices multiplication $O(mnp)$ where the first matrix of dimension is m×n, the second matrix is n×p and the matrices addition is$O(mn)$. Thus:

$$O(observer) = O(calculating\ \dot{\hat{X}}) + O(calculating\ \hat{Y}) + O(calculating\ r) =$$
$$[O(3\times3\times1) + O(3\times2\times1) + O(3\times1)] + [O(3\times3\times1) + O(3\times1)] = O(30)$$

Consequently, the complexity of the BNC is much better than the PO which is a plus. This comparison highlights the high capabilities of the BNC and subsequently, the eligibility of using Bayesian Belief Networks in the domain of fault detection and isolation within DC/DC power converters.

CONCLUSION AND PERSPECTIVES

This study discusses the ability of using Bayesian Belief Networks (BBN) in the domain of fault detection and isolation within DC/DC power converters via a comparative study between a simple, well-known and used FDI method represented by Proportional Observer (PO) versus the simplest form of the BBN represented by the Bayesian Naïve Classifier (BNC). Both methods were implemented and tested on real data. The BNC shows high advance on the PO in both latency and isolation accuracy. The isolation decision is supported by 99% confidence probability. This study will be extended in order to detect and isolate more faults, mainly the short circuit faults.Finally, the case of multi DC/DC converters will beconsidered by detecting the faulty DC/DC converter inside the SMSE (Fig. 1) followed by isolating the fault that occurs in this converter.

ACKNOWLEDGMENT

This study was supported by a grant from the Lebanese National Council for Scientific Research (no.01-07-11, LNCSR-3435/S).

REFERENCES

Bartram, G. and S. Mahadevan, 2013. Dynamic bayesian networks for prognosis. Proceeding of the Annual Conference of the Prognostics and Health Management Society.

Berendsen, C.S., G. Champenois, J. Davoine and G. Rostaing, 1992. How to detect and to localize a fault in a DC/DC converter? Proceeding of the International Conference on Industrial Electronics, Control, Instrumentation and Automation and Power Electronics and Motion Control. San Diego, CA, USA, pp: 536-541.

Colot, O., C. Olivier, P. Courtellemont and A. El Matouat, 1994. Information Criteria and Abrupt Changes in Probability Laws. In: Signal Processing VII: Theory and Applications, pp: 1855-1858.

Cowell, R., 1998. Introduction to Inference for Bayesian Networks. In: Jordan, M.I. (Ed.), Learning in Graphical Models. Springer, Netherlands, pp: 9-26.

Flores, M.J., A.E. Nicholson, A. Brunskill, K.B. Korb and S. Mascaro, 2011. Incorporating expert knowledge when learning Bayesian network structure: A medical case study. Artif. Intell. Med., 53(3): 181-204.

Friedman, N., D. Geiger and M. Goldszmidt, 1997. Bayesian network classifiers. Mach. Learn., 29(2-3): 131-163.

Gao, J., Y. Ji, J. Bals and R. Kennel, 2012. Fault detection of power electronic circuit using wavelet analysis in modelica. Proceeding of the 9th International MODELICA Conference. Munich, Germany, pp: 513-522.

Grossman, D. and P. Domingos, 2004. Learning bayesian network classifiers by maximizing conditional likelihood. Proceeding of the 21st International Conference on Machine Learning. Banff, Canada, pp: 46.

Guerin, F. and D. Lefebvre, 2009. Residual analysis for the diagnosis of hybrid electrical energy systems. IFAC P. Ser., 42(8): 1366-1371.

Guerin, F. and D. Lefebvre, 2013. Adaptive generalized PID controllers and fuzzy logic coordinator for load sharing in SMSE. Proceeding of the IEEE 52nd Annual Conference on Decision and Control (CDC, 2013). Firenze, Italy, pp: 5588-5593.

Guerin, F., C. Labarre and D. Lefebvre, 2011a. Magnetic near-field measurement for FDI of ZVS full bridge isolated buck converter. Proceeding of the IEEE International Symposium on Diagnostics for Electric Machines, Power Electronics and Drives (SDEMPED, 2011). Bologna, Italy, pp: 344-349.

Guérin, F., D. Lefebvre, A.B. Mboup, J.Y. Parédé, E. Lemains and P.A.S. Ndiaye, 2011b. Hybrid modeling for performance evaluation of multisource renewable energy systems. IEEE T. Autom. Sci. Eng., 8(3): 570-580.

Guerin, F., D. Lefebvre and V. Loisel, 2012. Supervisory control design for systems of multiple sources of energy. Control Eng. Pract., 20(12): 1310-1324.

Guo, H. and W. Hsu, 2002. A survey of algorithms for real-time Bayesian network inference. Proceeding of the AAAI/KDD/UAI02 Joint Workshop on Real-Time Decision Support and Diagnosis Systems. Edmonton, Canada.

Huang, C. and A. Darwiche, 1994. Inference in belief networks: A procedural guide. Int. J. Approx. Reason., 11(1): 158.

Jensen, F.V., 1996. An Introduction to Bayesian Networks. Vol. 210, UCL London.

Kamel, T., Y. Biletskiy, C.P. Diduh and L. Chang, 2015. Open circuit fault diagnoses for power electronic converters. Proceeding of the IEEE 24th International Symposium on Industrial Electronics (ISIE). Buzios, pp: 361-366.

Khanafer, R.M., B. Solana, J. Triola, R. Barco, L. Moltsen, Z. Altman and P. Lazaro, 2008. Automated diagnosis for UMTS networks using Bayesian network approach. IEEE T. Veh. Technol., 57(4): 2451-2461.

Kim, S.Y., K. Nam, H.S. Song and H.G. Kim, 2008. Fault diagnosis of a ZVS DC–DC converter based on DC-link current pulse shapes. IEEE T. Ind. Electron., 55(3): 1491-1494.

Langley, P., W. Iba and K. Thompson, 1992. An analysis of Bayesian classifiers. Proceeding of the 10th National Conference on Artificial Intelligence (AAAI, 1992), pp: 223-228.

Levin, K.T., E.M. Hope and A.D. Domínguez-Garcíay, 2010. Observer-based fault diagnosis of power electronics systems. Proceeding of the IEEE Energy Conversion Congress and Exposition (ECCE). Atlanta, GA, USA, pp: 4434-4440.

Madden, M.G., 2003. The performance of Bayesian network classifiers constructed using different techniques. Proceeding of the European Conference on Machine Learning, Workshop on Probabilistic Graphical Models for Classification, pp: 59-70.

Mboup, A.B., F. Guérin, P.A. Ndiaye and D. Lefebvre, 2008. Multimodel for the coupling of several dc/dc power converters on a dc bus. Proceeding of the IEEE International Symposium on Industrial Electronics (ISIE,2008). Cambridge, England, pp: 1507-1512.

Meziane, H., C. Labarre, S. Lefteriu, M. Defoort and M. Djmemai, 2015. Fault detection and isolation for a multi-cellular converter based on sliding mode observer. IFAC-PapersOnLine, 48(21): 164-170.

Pearl, J., 1988. Probabilistic Reasoning in Intelligent Systems: Networks of Plausible Inference. Kaufmann, San Mateo, California.

Pearl, J., 2000. Causality: Models, Reasoning and Inference. Cambridge University Press, Cambridge.

Redner, R.A. and H.F. Walker, 1984. Mixture densities, maximum likelihood and the EM algorithm. SIAM Rev., 26(2): 195-239.

Saad, A., I. Zaarour, A. Zeinedine, M. Ayache, P. Bejjani, F. Guerin and D. Lefebvre, 2013. A preliminary study of the causality of freezing of gait for parkinson's disease patients: Bayesian belief network approach. IJCSI Int. J. Comput. Sci. Issues, 10(3): 88-95.

Tiplica, T., S. Verron, A. Kobi and I. Nastac, 2006. FDI in multivariate process with naive bayesian network in the space of discriminant factors. Proceeding of the International Conference on Computational Intelligence for Modelling, Control and Automation and International Conference on Intelligent Agents, Web Technologies and International Commerce (CIMCA'06). Sydney, NSW, pp: 216-216.

Volosencu, C. and I.D. Curiac, 2010. Fault detection and diagnosis of distributed parameter systems based on sensor networks and Bayesian networks. Proceeding of the 6th WSEAS International Conference on Dynamical Systems and Control, pp: 167-173.

Wiegerinck, W., 2005. Modeling Bayesian Networks by Learning from Experts. Proceeding of the BNAIC, pp: 305-312.

Zaarour, I., A. Saad, A.Z. Eddine, M. Ayache, F. Guerin, P. Bejjani and D. Lefebvre, 2015. Methodologies for the Diagnosis of the Main Behavioral Syndromes for Parkinson's Disease with Bayesian Belief Networks. In: Tran, Q.N. and H. Arabnia (Eds.), Emerging Trends in Computational Biology, Bioinformatics and Systems Biology. Morgan Kaufmann, Boston, pp: 467-485.

Zein Eddine, A.H., I. Zaarour, F. Guerin, A. Hijazi and D. Lefebvre, 2015. Fault detection and isolation for ZVS full bridge isolated buck converter based on: Observer design and Bayesian network. Int. J. Adv. Res. Comput. Commun. Eng., 4(7): 242-249.

Zein Eddine, A., I. Zaarour, F. Guerin, A. Hijazi and D. Lefebvre, 2016. Improving fault isolation in DC/DC converters based with bayesian belief networks. Proceeding of the 4th IFAC International Conference on Intelligent Control and Automation Science (ICONS), France.

Zheng, F. and G.I. Webb, 2005. A comparative study of semi-naive bayes methods in classification learning. Proceeding of the 4th Australasian Data Mining Conference (AusDM05). Sydney, pp: 141-156.